Architecture and Performance of the Long Loop Algorithm for EGNOS V3 NLES Stations

Sergi Locubiche-Serra, *Universitat Autònoma de Barcelona (UAB), IEEC-CERES, Spain*

Marc Solé-Gaset, Miguel Á. Suárez-Gopar, *Indra Sistemas, Barcelona, Spain*

Nasser Zaidi, Arnault Sfeir, *Airbus Defence and Space, Toulouse, France*

Peter Claes, *European Space Agency (ESA), Toulouse, France*

Gonzalo Seco-Granados, José A. López-Salcedo, *Universitat Autònoma de Barcelona (UAB), IEEC-CERES, Spain*

BIOGRAPHIES

Dr. Sergi Locubiche-Serra received his M.Sc. and Ph.D. degrees in Telecommunications Engineering from Universitat Autònoma de Barcelona (UAB) in 2014 and 2019, respectively. He is currently working as a post-doctoral researcher and project engineer at UAB, and he is affiliated with the Institute of Space Studies of Catalonia (IEEC-CERES). He held a visiting appointment at the European Space Agency (ESA) in 2016. He has been involved in numerous projects funded by ESA and other national and international space-related entities on advanced positioning solutions for next-generation GNSS receivers.

Marc Solé-Gaset received his M. Sc. in Telecommunication Engineering specialized in Communications and his B. Degree in Aeronautics Engineering specialized in Aero-Navigation from Universtitat Politècnica de Catalunya (UPC) in 2009 and 2011, respectively. He is an expert GNSS Engineer with more than 12 years of professional experience in the field of satellite navigation. He has been involved in several working stages at Delft university of Technology (TUD), working on the development of classical as well as Advanced Receiver Autonomous Integrity Monitoring algorithms (RAIM/ARAIM). His main involvement up to 2016 has been focused on GNSS navigation applied to civil aviation. He has been technically coordinating several R&D projects in GNSS and actively participating in the definition of future Galileo OS and Galileo + GPS MOPS through the participation in EUROCAE WG-62. Since 2016, he has been working on the development of GNSS Ground Segment products, specially focused on the development of NLES and RIMS prototype products for EGNOS v3. He is currently the System Lead for NLES EGNOS v3 system and for the development of the NLES Long Loop Algorithm design.

Miguel Á. Suárez-Gopar received his B. Degree in Telecommunictions engineering specialized in telecommunications systems from Universidad de las Palmas de Gran Canaria (ULPGC) in 2018 and his M.Sc. in Aerospace Science and Technology from Universtitat Politècnica de Catalunya (UPC) in 2020. He has performed research for project Herakles (ULPGC+UPM) studying the propagation of acoustic and EM waves in the underwater channel. He has also collaborated with CTTC (Centre Tecnològic de Telecomunicacions de Catalunya) and INMARSAT doing research in the field of genetic algorithm and artificial intelligence used for the management and resources allocation of satellites' flexible payloads. Since 2020 he has been working as System and AIV engineer for the NLES EGNOS v3 system and for the development of the NLES Long Loop Algorithm design.

Nasser Zaidi received a M.Sc. degree in Communications Systems and Networking from ENSEEIHT at Toulouse in 1993 and a M.Sc. degree in Electronics, major in Microwave and Optical Communications from University of Limoges in 1986. He worked in the field of Navigation by Satellite Based Augmentation Systems (EURIDIS, EGNOS Testbed), as the uplink station technical manager from 1997 to 2000. He is currently working as the Technical Officer for the EGNOS V3 NLES. Nasser joined Airbus D&S in 2000 as ground system architect participating to satellite major programs for export, defense and institutional such as Eutelsat Quantum, Kmilsat, Measat 3BX, YahSat, French MoD telecoms programs, Falcon Eyes, Arabsat, ESA ARTES Programs from ground design definition until their on-site deployments.

Arnault Sfeir has worked more than 10 years in the field of Navigation by Satellite Based Augmentation Systems (SBAS, EGNOS), as the SBAS dissemination by Space and uplink station manager. He graduated as a Telecom Engineer from ENSEEIHT, Toulouse, and joined Thales Alenia Space in 1996 as satellite payloads AIV (Assembly, Integration and Validation) manager for 6 of them. He subsequently spent 4 years in French Guyana as Ariane 5 Telemetry Operations Manager, before managing the IOT (In-Orbit Test) monitoring system for the Globalstar 2 satellite constellation. Then he managed during 8 years the SBAS uplink stations (NLES G2 for EGNOS, SGS for KASS) from design definition until their on-site deployments. Joining Airbus in 2019, he is currently managing advanced projects in Navigation, in particular the rail H2020 CLUG proof of concept project leading the architecture and design of the Train Localisation On-Board Unit introducing GNSS and SBAS in European railway. He also supports the Airbus EGNOS-V3 project as SBAS space segment and NLES expert advisor.

Peter Claes received a M.Sc. degree in Electro-mechanical engineering from the University of Leuven (BE) in 1986, major in Microwave and Satellite Communication engineering. He also holds a Postgraduate degree in Computing for Commerce and Industry (U.K.) and a M.Sc degree in Geophysics and Astrophysics (Liège (BE)). He works for the European Space Agency (ESA) since 1993, first in two scientific projects as IVQ engineer and Operations Leader. Since 2001 he has been working in the Galileo Project in the Netherlands as development engineer responsible for the Archive, the Integrity subsystem, and the

https://doi.org/10.33012/2021.17883

Support Facilities. Since 2011 he is employed in the EGNOS Project in Toulouse, responsible for Data Dissemination (NLES), Monitoring and Control and supporting the Space Segment. Recently he is actively working on a R&D roadmap for future data dissemination for EGNOS.

Prof. Gonzalo Seco-Granados received the Ph.D. degree in Telecommunications Engineering from Universitat Politècnica de Catalunya (UPC) in 2000, and the MBA degree from IESE Business School in 2002. Until 2005 he was with ESA, involved in the design of the Galileo system. Since 2006 he has been with UAB as a Professor. He is also affiliated with the IEEC-CERES. In 2015 and 2019 he was a Fulbright Visiting Scholar with the University of California, Irvine. He is the Chair of the Spanish Chapter of the IEEE Aerospace and Electronic Systems Society (AESS). His research interests include the design of signals and reception techniques for satellite and terrestrial localization systems, multi-antenna receivers, and positioning with 5G technologies.

Prof. José A. López-Salcedo received his M.Sc. and Ph.D. degrees in Telecommunications Engineering from UPC in 2001 and 2007, respectively. Since 2006 he has been with UAB, where he is a Professor and also affiliated with the IEEC-CERES. He held visiting appointments at the University of Illinois Urbana-Champaign, the University of California Irvine, and the European Commission (EC) Joint Research Center (JRC). He is the Secretary/Treasurer of the Spanish Chapter of the IEEE Aerospace and Electronic Systems Society (AESS). His research interests lie in the field of statistical signal processing, including parameter estimation, statistical filtering and detection theory, with applications to GNSS receivers.

ABSTRACT

The third version of the European Geostationary Navigation Overlay Service (EGNOS V3) is a project that will provide Dual Frequency Multi-Constellation (DFMC) Satellite-Based Augmentation System (SBAS) services over Europe in the coming years. EGNOS V3 will augment the GALILEO and Global Positioning System (GPS) constellations, and improve robustness and enhance the performances of safety-of-life (SoL) services. The termed Navigation Land Earth Stations (NLES) are ground stations in charge of generating the SBAS signals and further transmitting them to a geostationary (GEO) satellite at C band, which then performs down-conversion to L band and broadcasts the resulting signals back to the Earth. Consequently, SBAS signals experience both uplink and downlink propagation effects if no further action is taken on them.

One of the key elements for successful operation in EGNOS V3 (and, in fact, in any SBAS system) is to accurately control signal emission at the output of the GEO satellite transmit antenna. More particularly, the objective is that the downlink SBAS signals be synchronized with the Global Navigation Satellite System (GNSS) signals commonly used for ranging purposes, which experience only the downlink effects from the satellites to the Earth. To this end, the Long Loop Algorithm (LLA) is a software integrated into the NLES stations that has been designed with a twofold purpose. First, to control GEO signal emission through the NLES signal generator and perform real-time steering of SBAS signals to virtually remove the uplink propagation effects from the NLES to the GEO output antenna. This is achieved by precisely determining the effects and delays to be eliminated, and further commanding the signal generator accordingly. And second, to do so while keeping coherence between code and carrier measurements, in order to be compliant with performance requirements stated by the International Civil Aviation Organization (ICAO).

The purpose of this paper is to present the LLA that has been designed for EGNOS V3 NLES stations. We describe the features of the software and the architecture of the algorithm, highlighting the use of more than one signal path to ensure proper LLA operation and the ability to operate in prediction mode in the absence of receiver measurements due to hardware malfunction for some seconds. The algorithm is formed by two consecutive blocks. On the one hand, the estimation module is used for determining the propagation effects to be eliminated. On the other hand, the control module is used for computing the corrections to be applied at the signal generator, based on the estimation module outputs.

I. INTRODUCTION

Satellite-based augmentation systems (SBAS) complement Global Navigation Satellite System (GNSS) signals with corrections and signal integrity information through additional messages broadcasted from geostationary (GEO) satellites. This includes certificates of safety for aviation users, error bounds for GNSS satellites and warning of rare system faults, to mention a few [1]. As a result, GNSS users benefit from enhanced positioning accuracy and robustness, with safety-of-life civil aviation applications in the spotlight. In that sense, the European Geostationary Navigation Overlay Service (EGNOS) is the system providing SBAS coverage across Europe. Its third version, referred to as EGNOS V3, is currently under development by the European Space Agency (ESA) contracting Airbus Defence and Space, and it will be deployed by the European Union Agency for the Space Programme (EUSPA) together with ESA and provide EGNOS services in the coming years.

EGNOS V3 will provide new Dual Frequency Multi-Constellation (DFMC) services for a multitude of user communities and will augment the GALILEO and Global Positioning System (GPS) constellations. Unlike the GNSS signals generated from the satellites orbiting the Earth, the EGNOS signal is generated from the Earth's ground in the Navigation Land Earth Station (NLES), a dual-frequency station that transmits the signal to a GEO satellite using the C1 and C5 band. Both signals are down-converted to L1 and L5 band by the GEO transponders, which then broadcast the resulting L1 and L5 signals back to the Earth, thus experiencing both uplink and downlink propagation effects.

One of the main functions of NLES stations is to perform real-time steering of the signals uplinked to the GEO satellites and control signal emission at the output of these latter. The aim is to make the signals generated from NLES stations look as if they are emitted from the GEO satellite, as occurs in GNSS signals, thus experiencing only the effects of the downlink from the satellite to the receiver. To this end, the problem is addressed by means of the so-called Long Loop Algorithm (LLA). It is one of the core elements of NLES V3 stations that is being designed and developed by the authors of this work from Institut d'Estudis Espacials de Catalunya at Universitat Autònoma de Barcelona (UAB, IEEC-CERES), in collaboration with Indra Sistemas, who is the main responsible for the hardware implementation, testing and validation, and Airbus Defence and Space being the EGNOS V3 system prime contractor. The LLA is an iterative algorithm designed with a twofold motivation. First, to determine and compensate for the propagation effects in the uplink path from the NLES to the GEO, so that the broadcasted signals be perceived as GNSS-like signals and, hence, made compatible with standard GNSS receivers. And second, to do so in a way to maintain coherence between code and carrier measurements of the EGNOS signals emitted from the GEO and be compliant with the Standards and Recommended Practices (SARPS) and performance requirements stated by the International Civil Aviation Organization (ICAO) [2].

The objective of this paper is twofold. First, to present an overview of design of the LLA for EGNOS V3 NLES stations. Second, to provide some preliminary results of its real-time steering performance for controlling signal emission at the output of the GEO transmit antenna. In Section II we state the problem to be addressed by the LLA, where an identification and description of the uplink propagation effects and delays to be eliminated is provided. Special emphasis is placed on their impact at physical level onto code and carrier measurements, as some effects do not affect both types of measurements equally and thus introduce code-carrier incoherence.

Section III describes the general architecture of the proposed algorithm, where additional calibration paths are introduced to ensure LLA functionality. In particular, to ensure visibility of the undesired propagation effects, and to provide the LLA with a memory effect on the corrections applied up to the current time instant. Additionally, the blocks constituting the LLA core from the algorithmic standpoint, namely the estimation and control modules, are briefly described, introducing the beauty of the designed algorithm, which is the ability of operating in prediction mode. That is, to keep providing controls and steering the uplink signals in the absence of receiver measurements, caused by any kind of hardware malfunction for some seconds or even minutes.

Section IV shows preliminary results on the steering performance of the proposed LLA. Two types of results are provided. First, a full software simulator has been implemented in MATLAB to perform a preliminary validation of the algorithm design and evaluate the fulfillment of the ICAO SARPS and performance requirements. Results on the signals emitted at the simulated GEO output without and with LLA controls are shown. And second, experimental results with real hardware are provided. At this stage of project development, the LLA operation is confirmed by means of an NLES prototype that has been built at Indra's premises, together with a GEO payload simulator, where we compare the post-LLA downlink with the expected one, the one that should be theoretically observed. Last, this section also shows some preliminary results on the ability of the LLA to operate in prediction mode. Section V draws the conclusions.

II. PROBLEM STATEMENT

The general architecture of NLES V3 stations is illustrated in Figure 1. The chain is composed of three main blocks. First, the transmission side is formed by the signal generator, which outputs the signal at intermediate frequency (IF), and it is followed by a transmission conditioning block accommodating an IF-to-C band up-converter (UC) and a high-power amplifier (HPA). The resulting signal is uplinked to the GEO by means of a directive antenna. Second, the signal-in-space (SiS) block encompasses all the uplink and downlink propagation effects experienced by the SBAS signal, plus the effects and delays of the GEO payload, which down-converts (DC) the uplinked signal from C to L band prior to broadcasting. And third, the reception side is composed of another directive antenna for receiving the signal coming from the GEO, followed by the radio-frequency (RF) front-end signal conditioning including low-noise amplifiers and filters. Then, the receiver provides pseudorange (*i.e.* code) and carrier phase measurements at L1 and L5 bands.

In that sense, the LLA is the chain element that closes the loop in Figure 1 by acting as the link connecting the reception and transmission sides of the NLES. By capturing and processing the signal broadcasted by the GEO satellite, the algorithm determines the uplink effects to be cancelled out and controls GEO signal emission. In practical terms, the ultimate objective is to observe zero delay and dynamics at the GEO output. This is achieved by commanding a signal advance to the signal generator in the opposite direction to the undesired uplink. In this way, when the actual uplink is added up during signal travel, it ends up being eliminated and the signals appear as if they are generated onboard the GEO satellite.

1. Description of Propagation Effects

The first step in formulating the LLA problem is to identify the delays and propagation effects that are to be eliminated (*i.e.* uplink) and distinguish them from those that are to remain untouched (*i.e.* downlink). Furthermore, it is of paramount importance to specify how they affect the different measurement types and thus contribute to code-carrier incoherence. In that sense, the following is a list of the identified effects in the chain in Figure 1 [3]:

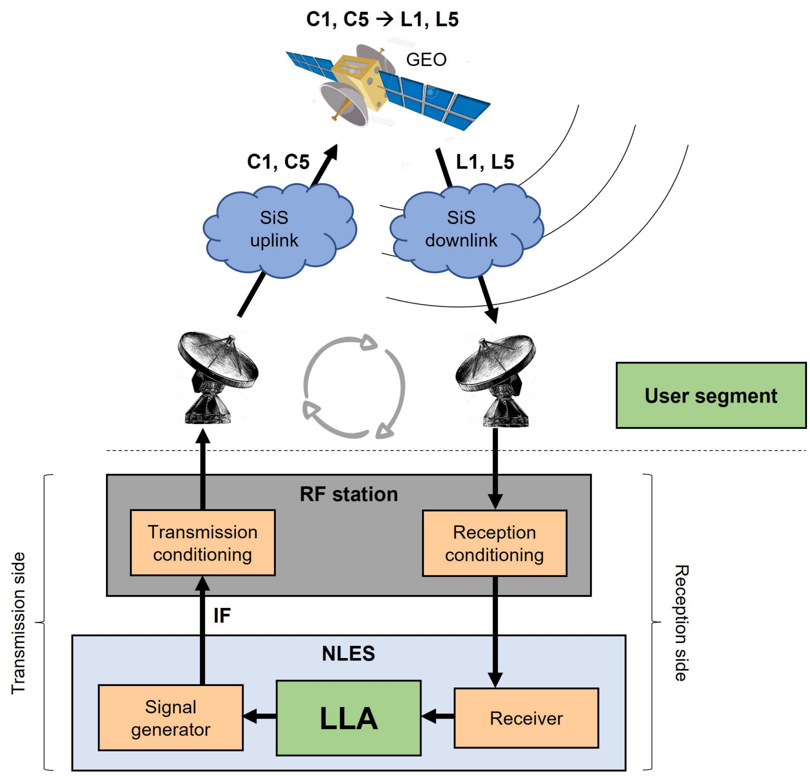

Figure 1: General description of NLES functionality for EGNOS V3 integrating LLA for signal steering.

- **Satellite range and orbit dynamics**: it is the physical distance between the NLES and the GEO plus residual satellite dynamics, usually following a one-day-period sine wave-like shape. This effect is equally present in both pseudorange and carrier phase measurements. It is perceived twice due to the presence of both uplink and downlink paths, and thus the former can be compensated by removing half of it.
- **Tropospheric delay**: it is the delay introduced when crossing the Earth's troposphere. It is not a dispersive effect, meaning that the impact is the same at the uplink and downlink paths of both pseudorange and carrier phase measurements, irrespective of the carrier frequencies. Hence, it will be perceived as part of the satellite range.
- **Ionospheric delay**: it is the time-varying delay introduced by the Earth's ionosphere, and it can reach up to 25 meters in the vertical direction [4]. In contrast to the troposphere, the ionosphere is dispersive, thus introducing code-carrier incoherence. On the one hand, it delays the code phase and advances the carrier phase. On the other hand, its impact is dependent on the carrier frequencies, meaning that the delays will be different in the uplink and downlink and between bands C1, C5, L1 and L5.
- **Hardware delays**: they refer to the insertion delays introduced by the different hardware elements in the chain, namely UC, GEO payload, filters, amplifiers and wiring. They affect all measurements equally within a frequency band, and do not cause code-carrier divergence.
- **Frequency translation error**: it is the systematic error introduced when up-converting and down-converting the signals due to NLES and GEO oscillator inaccuracies. It affects only carrier phase measurements, and contributes hence to code-carrier divergence.
- **Phase noise**: a noise component of the local oscillator leads the frequency translation error to present a fluctuating behavior or random drift. It also affects only carrier phase measurements.
- **Inter-frequency delay**: referring to delta hardware delays at band C5/L5 with respect to the delays at frequencies C1/L1, it introduces signal incoherence between bands C1/L1 and C5/L5.
- **Phase wind-up effect**: it is a delay that depends on the relative orientation of the satellite and receiver antennas, the direction of the line of sight, and the satellite's orbital motion. The satellite must perform a rotation to keep its solar panels pointing towards the Sun while its antennas keep pointing towards the Earth. This rotation causes a phase variation that is misunderstood as an additional delay. Phase wind-up affects only carrier phase measurements.

- **Sagnac effect**: it is an additional delay owing to the Earth's rotation during signal travel to and from GEO. It makes the uplink and downlink range not to be exactly the same, and affects all measurements equally.
- **Pseudorange ripple**: pseudorange measurements from GEO satellites present an unwanted oscillation effect attributable to systematic receiver errors and dependent on Doppler and PRN [5, 6]. These oscillations can reach peak values of up to ± 0.5 meters, and whereas they are not to be corrected since these do not exist at the output of the GEO satellite (but are inevitably originated at receiver side), they enter the LLA from all loops, and thus the controls become affected by an unwanted oscillatory behaviour. This effect is detrimental in pseudoranges at L1, whereas the effect in L5 is much milder and less problematic. Hence, we will focus only on the pseudorange ripple at L1.
- **Clock offset**: the NLES measurements are referred to the NLES time reference, which may present an offset with respect to the SBAS Network Time (SNT). This is an additional offset that must be taken into account to steer the signals to SNT.

2. Impact of Propagation Effects onto Code and Carrier Measurements

As anticipated in Section II.1, some of the above effects introduce code-carrier incoherence, as they do not affect pseudorange and phase measurements in the same manner. In that sense, the measurement equations perceived by the NLES receiver in Figure 1 and provided to the LLA are formulated as follows.

On the one hand, the discrete-time pseudorange measurements at L1 and L5 are:

$$\rho_{\mathrm{L1}}(n) = b_{\mathrm{L1}} + 2\left[r(n) + T(n)\right] + \left[I_{\mathrm{C1}}(n) + I_{\mathrm{L1}}(n)\right] + o(n) + \Sigma^{(c)}_{\rho_{\mathrm{L1}}}(n) + w_{\rho_{\mathrm{L1}}}(n) \tag{1}$$

$$\rho_{\mathrm{L5}}(n) = b_{\mathrm{L1}} + 2\left[r(n) + T(n)\right] + \left[I_{\mathrm{C5}}(n) + I_{\mathrm{L5}}(n)\right] + b_{\mathrm{L1\text{-}L5}} + \Sigma^{(c)}_{\rho_{\mathrm{L5}}}(n) + w_{\rho_{\mathrm{L5}}}(n) \tag{2}$$

in meters, where:

- b_{L1} is the aggregate hardware delays in the chain experienced by the pseudorange at C1/L1 band including the UC, HPA, GEO payload and lever arm, Sagnac effect, receiver front-end and wiring;
- $r(n)$ is the NLES-to-GEO geometric distance plus GEO dynamics;
- $T(n)$ is the tropospheric delay;
- $\{I_{\mathrm{C}j}(n), I_{\mathrm{L}j}(n)\}$ are, respectively, the uplink and downlink ionospheric delays at frequency j, with $j = \{1, 5\}$;
- $o(n)$ is the oscillation (*i.e.* ripple) effect experienced in the pseudorange measurement at L1;
- $b_{\mathrm{L1\text{-}L5}}$ is the inter-frequency delay, the delta delay experienced at L5 with respect to the delay at L1;
- $\Sigma^{(c)}_{\rho_{\mathrm{L}j}}(n)$ is the accummulated corrections applied at the signal generator for each pseudorange measurement;
- $w_{\rho_{\mathrm{L}j}}(n)$ is the pseudorange measurement noise.

At this point, it is interesting to note that the ionospheric delays experienced at the different carrier frequencies are inter-proportional, meaning that all values can be obtained by applying scaling factors to only one of them. We have selected the downlink ionospheric delay at L1, from which the rest of delays are computed by scaling through a carrier frequency-dependent factor α. Therefore, the pseudorange measurements in (1) and (2) can be rewritten as,

$$\rho_{\mathrm{L1}}(n) = b_{\mathrm{L1}} + 2\left[r(n) + T(n)\right] + \left(\alpha_{\rho_{\mathrm{C1}}} + \alpha_{\rho_{\mathrm{L1}}}\right) I_{\mathrm{L1}}(n) + o(n) + \Sigma^{(c)}_{\rho_{\mathrm{L1}}}(n) + w_{\rho_{\mathrm{L1}}}(n) \tag{3}$$

$$\rho_{\mathrm{L5}}(n) = b_{\mathrm{L1}} + 2\left[r(n) + T(n)\right] + \left(\alpha_{\rho_{\mathrm{C5}}} + \alpha_{\rho_{\mathrm{L5}}}\right) I_{\mathrm{L1}}(n) + b_{\mathrm{L1\text{-}L5}} + \Sigma^{(c)}_{\rho_{\mathrm{L5}}}(n) + w_{\rho_{\mathrm{L5}}}(n). \tag{4}$$

On the other hand, the discrete-time carrier phase measurements are as follows:

$$\varphi_{\mathrm{L1}}(n) = b_{\mathrm{L1}} + 2\left[r(n) + T(n)\right] - \left[I_{\mathrm{C1}}(n) + I_{\mathrm{L1}}(n)\right] + \theta_{\mathrm{L1}}(n) - K_{\mathrm{L1}} + \Sigma^{(c)}_{\varphi_{\mathrm{L1}}}(n) + w_{\varphi_{\mathrm{L1}}}(n) \tag{5}$$

$$\varphi_{\mathrm{L5}}(n) = b_{\mathrm{L1}} + 2\left[r(n) + T(n)\right] - \left[I_{\mathrm{C5}}(n) + I_{\mathrm{L5}}(n)\right] + \theta_{\mathrm{L5}}(n) + b_{\mathrm{L1\text{-}L5}} - K_{\mathrm{L5}} + \Sigma^{(c)}_{\varphi_{\mathrm{L5}}}(n) + w_{\varphi_{\mathrm{L5}}}(n) \tag{6}$$

also expressed in meters, with some terms in common with pseudorange measurements, but with the following additional effects affecting only carrier phase:

- $\theta_{\mathrm{L}j}(n)$ is the aggregate UC plus GEO phase error owing to frequency translation errors, oscillator phase noise and phase wind-up effect;
- $\Sigma^{(c)}_{\varphi_{\mathrm{L}j}}(n)$ is the accummulated corrections applied at the signal generator for each carrier phase measurement;
- $K_{\mathrm{L}j}$ is the initial carrier phase ambiguity;

- $w_{\varphi_{\mathrm{L}j}}(n)$ is the carrier phase measurement noise.

When using a common local oscillator, the phase error $\theta_{\mathrm{L5}}(n)$ is proportional to the phase error $\theta_{\mathrm{L1}}(n)$ through the scaling factor $\alpha_\theta \doteq \frac{f_{\mathrm{C5}}-f_{\mathrm{L5}}}{f_{\mathrm{C1}}-f_{\mathrm{L1}}}$. Therefore, together with the scaling factors of the ionospheric delays, the carrier phase measurements in (5) and (6) can be rewritten as,

$$\varphi_{\mathrm{L1}}(n) = b_{\mathrm{L1}} + 2\left[r(n) + T(n)\right] - \left(\alpha_{\varphi_{\mathrm{C1}}} + \alpha_{\varphi_{\mathrm{L1}}}\right) I_{\mathrm{L1}}(n) + \theta_{\mathrm{L1}}(n) - K_{\mathrm{L1}} + \Sigma^{(c)}_{\varphi_{\mathrm{L1}}}(n) + w_{\varphi_{\mathrm{L1}}}(n) \tag{7}$$

$$\varphi_{\mathrm{L5}}(n) = b_{\mathrm{L1}} + 2\left[r(n) + T(n)\right] - \left(\alpha_{\varphi_{\mathrm{C5}}} + \alpha_{\varphi_{\mathrm{L5}}}\right) I_{\mathrm{L1}}(n) + \alpha_\theta\theta_{\mathrm{L1}}(n) + b_{\mathrm{L1\text{-}L5}} - K_{\mathrm{L5}} + \Sigma^{(c)}_{\varphi_{\mathrm{L5}}}(n) + w_{\varphi_{\mathrm{L5}}}(n). \tag{8}$$

Last, the LLA is provided with a fifth measurement corresponding to the NLES clock offset with respect to SNT,

$$\Delta t(n) \doteq b_{clk}(n) + w_{\Delta t}(n) \tag{9}$$

which is used to steer the measurements in (3), (4), (7), (8) to SNT.

III. DESCRIPTION OF THE LONG LOOP ALGORITHM FOR EGNOS V3

This section describes the general architecture for the LLA V3 to achieve the targeted goal. From the software standpoint, the LLA is composed of two main blocks, namely the estimation module and the control module. The estimation module is in charge of determining the propagation effects to be counteracted at the signal generator based on the information provided by the receiver measurements. The control module computes the controls to be commanded based on the estimation module outputs and the precedent corrections that have been applied so far at the signal generator.

With both in mind, the first consideration at this point is that LLA operation cannot be achieved by feeding into the algorithm only the measurements in (3), (4), (7), (8), henceforth termed *long loop* measurements. The main reason is that these measurements do carry a combination of both the propagation effects to be determined and the accumulated corrections applied at the signal generator, and the consequence is twofold. On the one hand, the accumulated corrections distort the proper identification of the propagation effects, thus voiding the estimation module. On the other hand, at the same time, the propagation effects distort the retrieval of any information about the corrections accumulated at the signal generator. Consequently, no information about the corrections that remain to be applied can be extracted, thus voiding the control module. Therefore, additional actions must be taken at both software and hardware levels.

The proposed solution to the above issues adopted in LLA V3 is to introduce two additional signal paths, corresponding to the orange (2) and purple (3) paths in Figure 2 and henceforth termed *middle loop* and *short loop*, respectively. These are calibration signals, also referred to in this paper as *loopback* signals. As such, they come from the signal generator but do not travel into space. Instead, they are fed back into the NLES after transmission conditioning, and the rationale is to exploit the fact that they carry the accumulated signal generator corrections but not the SiS effects.

Thanks to the latter, the estimation module benefits from the middle loop by subtracting the corrections from the long loop, which are common in both paths, while leaving the SiS effects practically untouched. By performing such pre-conditioning of the estimation module inputs, the effects of interest become visible and the module can interestingly operate irrespective of the controls applied by the algorithm, thus avoiding any kind of LLA self-interference onto SiS determination. On the other hand, thanks to the short loop measurements, the control module can seize information about the corrections made so far by the signal generator, and it can therefore determine the corrections that remain to be applied in an intelligent manner, thus introducing a memory effect on the controls previously applied by the LLA.

In addition, it is observed that the middle and short loops are very similar paths, with the only difference that the latter does not carry the effects and delays on the reception side. The beauty of this two-link separation is that the estimation module benefits from the middle loop by also subtracting these effects that are common with the long loop and are indeed not to be compensated by the LLA, as well as these do not enter the loop from the short loop either.

IV. LLA PERFORMANCE RESULTS

Once the LLA architecture has been presented, in this section we show some results on the performance of the designed algorithm.

1. MATLAB Simulation Results

We start first by showing preliminary results obtained from a LLA simulator that has been built in MATLAB. Based on realistic GEO ephemeris data, the GEO orbit is assumed to follow a 1-day-period sine-wave shape located at a distance of 38400 km above the Earth surface with 48 km peak-to-peak distance. This is illustrated in Figure 3a top, which depicts the observed pre-LLA pseudoranges at the output of the GEO satellite. The ascending trend is due to the clock offset, which is given by the black dotted-striped line in the figure. The rest of delays (tropospheric delay, constant hardware delays) are placed together with the

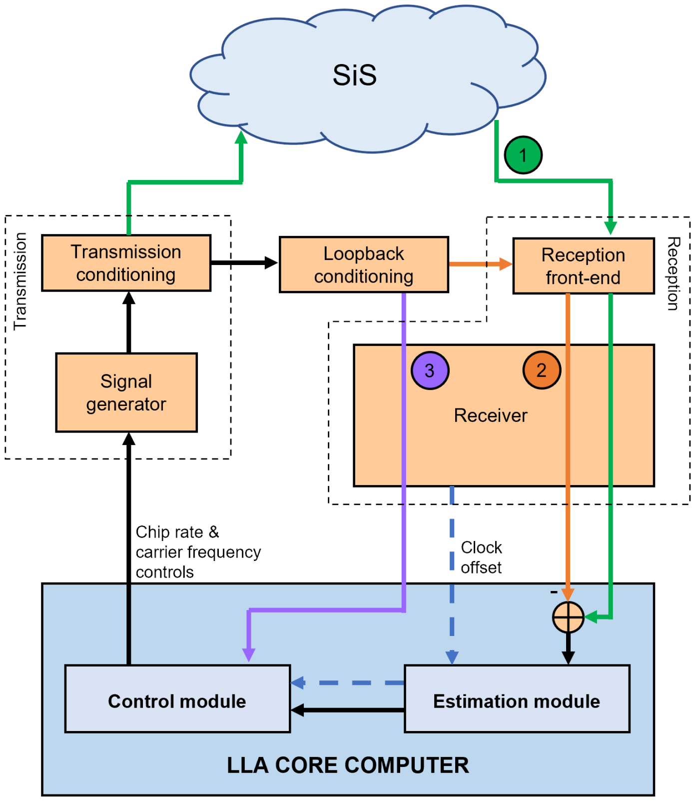

Figure 2: General architecture of NLES V3 stations integrating LLA for signal steering.

GEO orbit. We emphasize the ionospheric and inter-frequency delays, which are the parameters differentiating pseudoranges at L1 versus L5 as illustrated in Figure 3a bottom. Introducing a constant offset of around 2 m, the ionosphere follows the shape observed in the figure, on top of an inter-frequency delay that has been set to 50 meters [3]. On the other hand, Figure 3b depicts the observed pre-LLA carrier phase dynamics (*i.e.* Doppler) at the output of the GEO satellite. These are also affected by the above effects, particularly the sine-wave-shaped GEO orbit, placed on top of a NLES+GEO L1-to-C1-to-L1 frequency translation error obtained by assuming 1 ppb error for the NLES oscillator and 1 ppm error for the GEO one. In all loops, the carrier-to-noise ratio (C/N_0) at the receiver side is assumed to be 60 dB-Hz.

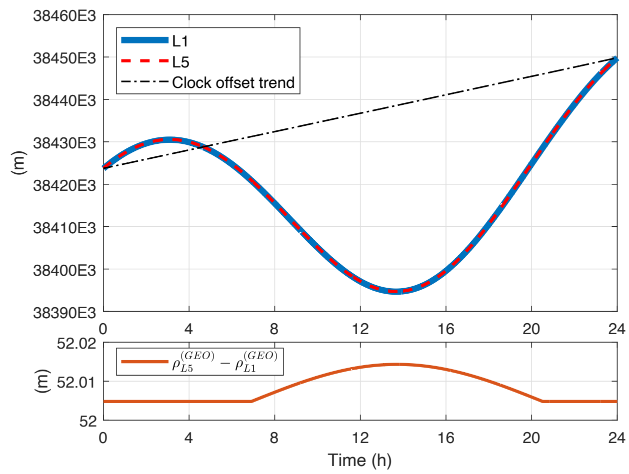

(a) (Top) Pseudorange measurements. (Bottom) Difference between pseudoranges at L1 and L5.

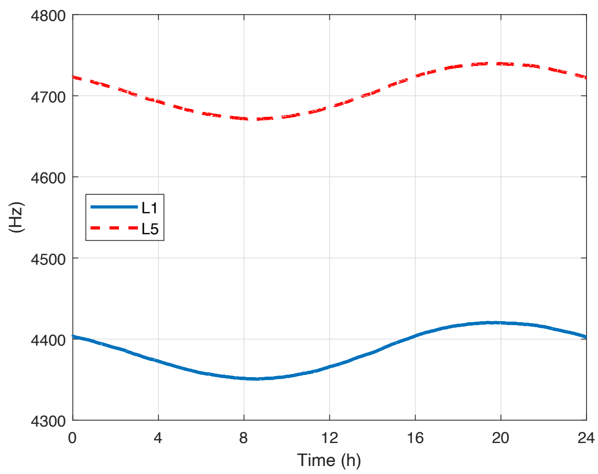

(b) Carrier phase dynamics.

Figure 3: Uncorrected measurements at output of GEO satellite transmit antenna.

Figures 4a and 4b are the post-LLA counterparts of previous Figures 3a and 3b. That is, the corrected measurements that are observed at the GEO satellite output with the LLA in operation. On the one hand, the pseudoranges are driven to a constant value, that is, no dynamics are observed at the GEO output, thus achieving the desired functionality. The delay departs from the ideal zero, though. The reason is that there is a small amount of delays in the chain which cannot be identified by the LLA, and thus remain as unidentified residual biases after LLA operation. This phenomenon was indeed foreseen as one baseline of the project, and hence an ICAO performance requirement is explicitly devoted to this topic, which states that the uncorrected residual biases should not exceed the green stripped line in Figure 4a. If otherwise, note that these biases can be pre-calibrated prior to LLA operation and further compensated by applying a manual correction in the algorithm, in order to be compliant with the above requirement. On the other hand, the carrier phase measurements observed at the GEO output also present zero dynamics as desired. Based on the above observations, the LLA V3 is concluded to perform successfully at simulation level.

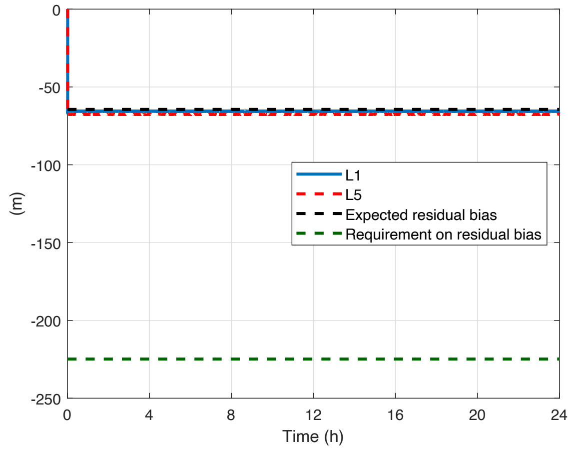

(a) Pseudorange measurements.

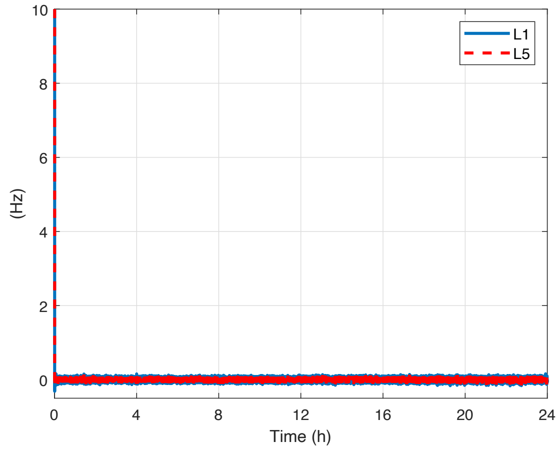

(b) Carrier phase dynamics.

Figure 4: Corrected measurements at output of GEO satellite transmit antenna.

2. Experimental Results on Indra's Platform

We now present experimentation results on Indra's platform with real hardware. The block diagram of the built platform is shown in Figure 5. Two features stand out. First, the use of a simulator for the GEO payload. Second, the use of a multi-frequency antenna (MFA) capturing GPS and Galileo signals for further computation of the NLES-to-SNT clock offset.

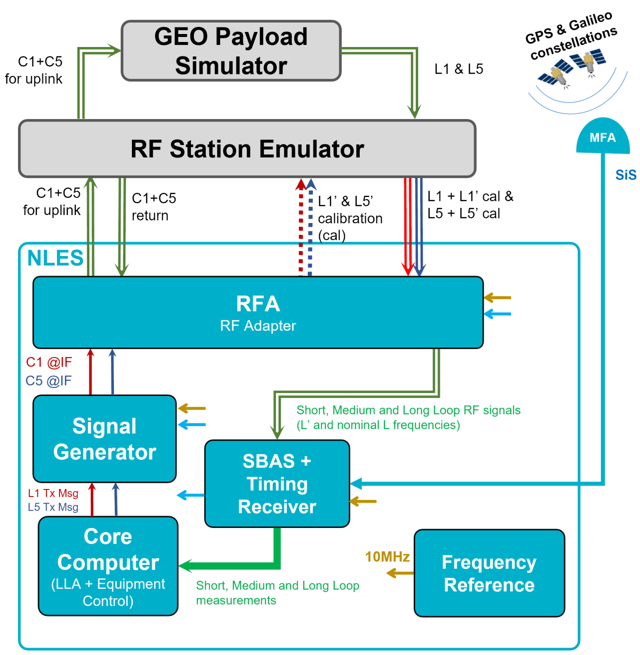

Figure 5: General overview of Indra's platform.

For an experimental test of a bit less than 12 hour duration, Figure 6 top shows the loopback errors for the pseudoranges at L1 and L5, whereas Figure 6 shows the dynamics of the carrier phase loopback errors. As can be observed, both are zero mean and kept as such over time, meaning that the LLA is correcting what it is told to, and no portion of signal remains to be eliminated. However, the ultimate proof on the correctness and performance of the algorithm is to compare the expected (*i.e.* theoretical) GNSS-like downlink and the measured one when the LLA is in operation. This is depicted in Figures 7a and 7b for pseudorange and Doppler measurements, respectively. The bottom plots show the difference between the theoretical and measured profiles. It is observed that the measurements do match the theoretical profiles, with a constant error in the pseudoranges and zero-mean Doppler error. This proves that the LLA can perform real-time steering of the time-varying propagation effects and GNSS-like signals are observed at the downlink as desired.

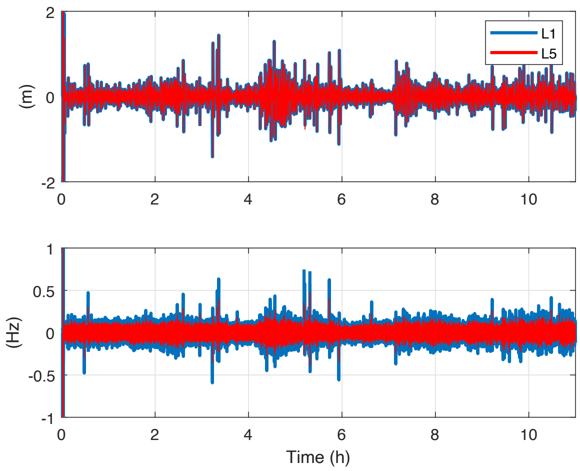

Figure 6: (Top) Pseudorange loopback errors. (Bottom) Carrier phase loopback error dynamics.

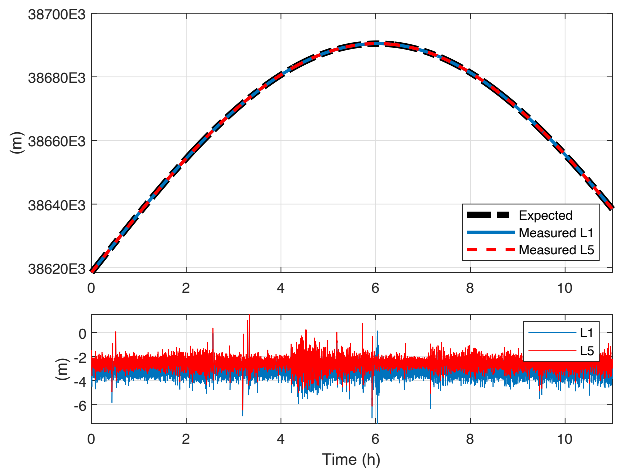

(a) Pseudorange measurements.

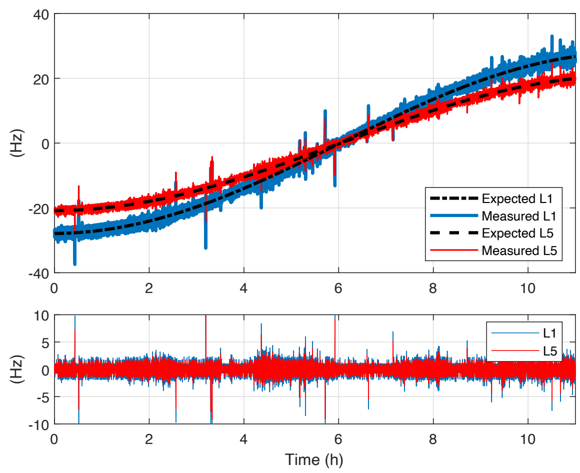

(b) Dynamics of carrier phase measurements.

Figure 7: (Top) Expected vs. measured downlink with LLA operating on Indra's platform. (Bottom) Difference between both.

3. Fulfillment of Performance Requirements

Table 1 compares the requirement metrics obtained in the MATLAB simulation environment and the experimentation results on Indra's platform. In few words, the code-carrier coherence (CCC) metric measures the misalignment between pseudorange and carrier phase observables within a window of 3600 seconds for the short term and 86400 seconds for the long term. Similarly, the code-carrier frequency coherence (FreqCoh) metric measures the misalignment between the variations of pseudorange and carrier phase observables within a period of 10 seconds for the short term and 100 seconds for the long term. As can be observed, all metrics are located below the requirement thresholds shown in the same table, thus preliminarily concluding that the designed LLA V3 successfully performs the task for which it has been conceived. Note that these results may vary depending on the simulated scenario and conditions (satellite orbit, GEO satellite performances, etc.).

Table 1: Performance requirement metrics obtained in MATLAB simulation environment and real hardware on Indra's platform.

ID	Threshold	MATLAB sim.	Indra's platform	Observations
Short-term CCC @L1	< 0.150 m	0.028 m	0.035 m	-
Short-term CCC @L5	< 0.200 m	0.041 m	0.028 m	
Long-term CCC @L1	< 0.190 m	0.059 m	0.121 m	
Long-term CCC @L5	< 0.255 m	0.084 m	0.108 m	
Short-term FreqCoh @L1	$< 5 \cdot 10^{-11}$	$1.366 \cdot 10^{-11}$	$1.784 \cdot 10^{-11}$	1-sigma
Short-term FreqCoh @L5		$1.957 \cdot 10^{-11}$	$1.489 \cdot 10^{-11}$	
Long-term FreqCoh @L1	< 0.190 m	0.087 m	0.173 m	
Long-term FreqCoh @L5	< 0.255 m	0.125 m	0.152 m	
LLA convergence	< 120 s	N/A	~ 45 s	As soon as receiver reacquires

4. LLA operation in prediction mode

As explained earlier, the most attractive feature of the designed LLA is the ability to operate in prediction mode in the absence of receiver measurements for some seconds. In that sense, Figure 8 depicts an example of the impact of signal outages in steady state causing the LLA to enter prediction mode onto the CCC requirement at both L1 and L5. Two outage durations have been considered, namely 60 and 70 seconds. As can be observed, the impact is given particularly in terms of the short-term CCC, which exceeds the threshold for a 70-second outage, whereas it can remain below the threshold if the outage lasts for 60 seconds. Therefore, as a preliminary result at this stage of the project, the LLA demonstrates to withstand signal outages of up to a minute duration without compromising requirement fulfillment. Note that, although exceeding the requirement thresholds, the LLA can still withstand outages of some minutes and recover from prediction mode afterwards.

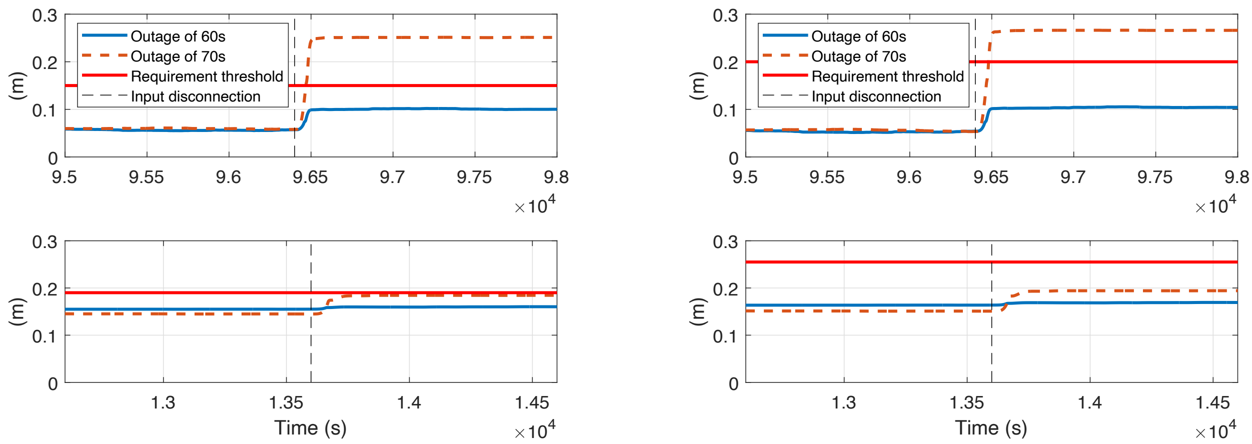

(a) Results for L1. **(b)** Results for L5.

Figure 8: Demonstration of LLA operation in prediction mode. (Top) Short-term CCC metric in the presence of signal outages of 60s and 70s duration. (Bottom) Long-term CCC.

V. CONCLUSIONS

EGNOS V3 is currently being developed as the successor of EGNOS V2 to provide modern SBAS services across Europe for the coming years. In that sense, this paper has presented the Long Loop Algorithm that has been designed for NLES V3 stations to steer the signals uplinked to the GEO satellite and manipulate the satellite-to-ground downlink in order to perceive GNSS-like signals. The architecture of the LLA has been shown, highlighting the use of calibration signals to clearly visualize the effects to be eliminated and to seize memory on preceding applied corrections. The ability to work in prediction mode and keep providing SBAS service continuity in the presence of hardware malfunction has been presented as the key enabling feature of our LLA.

Preliminary MATLAB simulation results and real-hardware experimentation tests have concluded on the correctness and performance of the proposed LLA and its ability to perform steering in real time by tracking the time evolution of the undesired effects and applying the corresponding controls to keep the loopback errors at zero. The LLA achieves the desired functionality by eliminating signal dynamics at the GEO output and, up to now, the algorithm is being demonstrated to be compliant with the ICAO SARPS.

ACKNOWLEDGEMENTS

This work has been carried out with the funding of the European Union.

DISCLAIMER

The views expressed herein can in no way be taken to reflect the official opinion of the European Union, the EU Agency for the Space Programme or the authors' organizations.

REFERENCES

[1] J. Rife, "WAAS Functions and Differential Biases. Do GNSS augmentation systems certified for aviation use, such as WAAS, have a function other than improving the accuracy of user navigation?" *Inside GNSS*, pp. 18–21, Jun 2008.

[2] International Civil Aviation Organization (ICAO), "DFMC SBAS SARPS - Part B, version 2.1."

[3] A. J. Van Dierendonck, R. Coker, O. Razumovsky, D. Bobyn, and H. Kroon, "Inmarsat-4 navigation transponder test equipment and control software for in-orbit tests," in *Proceedings of the 16th International Technical Meeting of the Satellite Division of The Institute of Navigation (ION GPS/GNSS 2003)*, 2003, pp. 1307–1319.

[4] B. Arbesser-Rastburg, *The challenge of the ionosphere for EGNOS*, 12 2006, vol. 1303, pp. 71 – 81.

[5] D. Borio, C. Gioia, and N. Mitchison, "Identifying a low-frequency oscillation in Galileo IOV pseudorange rates," *GPS Solutions*, vol. 20, no. 3, pp. 363–372, 2016.

[6] S. D. Ericson, "SBAS Signal in Space Performance Improvement through Code Phase Resolution Error Correction," in *Proceedings of the ION 2013 Pacific PNT Meeting*, 2013, pp. 995–1002.

ION GNSS+ 2021

Architecture and Performance of the Long Loop Algorithm for EGNOS V3 NLES Stations

S. Locubiche-Serra[1], M. Solé-Gaset[2], M. Á. Suárez-Gopar[2],
N. Zaidi[3], A. Sfeir[3], G. Seco-Granados[1], J. A. López-Salcedo[1]

UAB Universitat Autònoma de Barcelona [1]
IEEC Institut d'Estudis Espacials de Catalunya
indra [2]
AIRBUS DEFENCE & SPACE [3]

34th International Technical Meeting of the Satellite Division of the Institute of Navigation (ION GNSS+ 2021), September 20-24, 2021
https://doi.org/10.33012/2021.17883

Outline

1. Introduction and objectives
2. Problem statement
3. Architecture of the Long Loop Algorithm (LLA)
4. Estimation module and control module
5. Experimentation results and performance evaluation
6. Conclusions and on-going work

Outline

1. Introduction and objectives
2. Problem statement
3. Architecture of the Long Loop Algorithm (LLA)
4. Estimation module and control module
5. Experimentation results and performance evaluation
6. Conclusions and on-going work

Satellite-Based Augmentation Systems

- Satellite-based augmentation systems (SBAS) complement Global Navigation Satellite System (GNSS) signals with corrections and signal integrity information through additional messages broadcasted from geostationary (GEO) satellites.

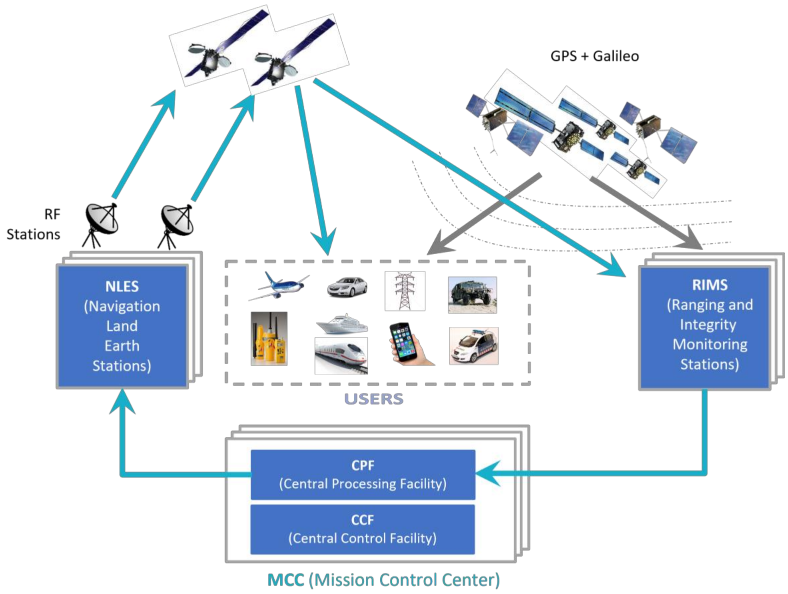

- Certificates of safety for aviation users, error bounds for GNSS satellites, warnings of rare system faults.
- Accuracy enhancement of GNSS-based ranging, with safety-of-life (SoL) civil aviation applications in the spotlight.

European Geostationary Navigation Overlay Service

EGNOS

- ❑ The third version of the European Geostationary Navigation Overlay Service (EGNOS V3) is under development as part of the modernization program promoted by the European Union Agency for the Space Programme (EUSPA) to provide European SBAS coverage for the coming years.

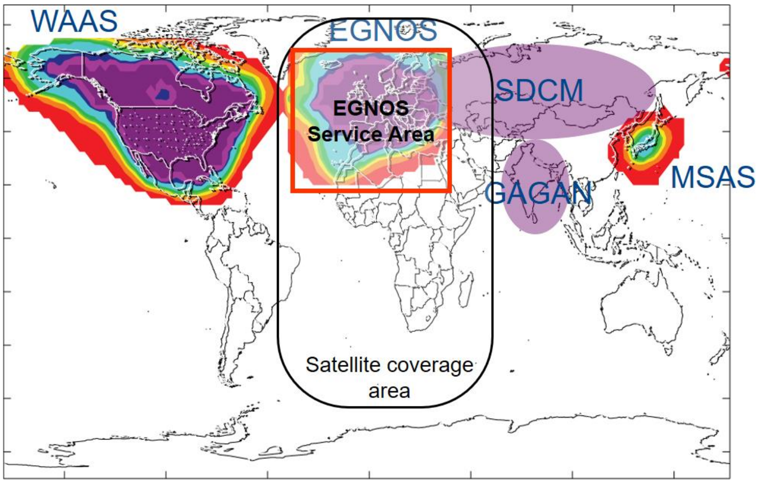

EGNOS **V3** *vs.* EGNOS **V2**

- ✓ Addition of GPS L5 and Galileo E1/E5 toward a dual-frequency multi-constellation (DFMC) concept.
- ✓ Enhanced vertical guidance accuracy and robustness.
- ✓ New services for new users (targeting safe maritime and railway navigation).
- ✓ Backwards compatibility with current GPS L1 in EGNOS V2.

SPCOMNAV Signal Processing for Communications and Navigation
Universitat Autònoma de Barcelona School of Engineering UAB

NLES and Long Loop Algorithm

- ❑ The purpose of NLES stations is to:
  - ➢ Transmit EGNOS corrections to the GEO, so it can broadcast them to EGNOS users.
  - ➢ Steer transmitted signals, so they are coherent according to International Civil Aviation Organization (ICAO) standards.

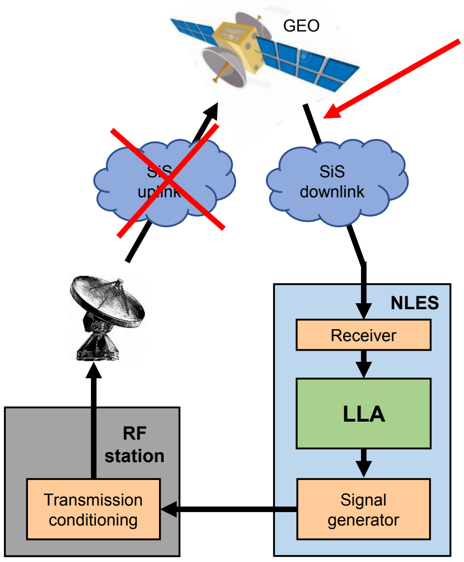

GNSS-like signals: zero delay and dynamics must be observed at this point.

SBAS signals encompass both **uplink** and **downlink** signal-in-space (SiS) delays and propagation effects.

LONG LOOP ALGORITHM (LLA)

- ✓ To steer EGNOS V3 signals uplinked to the GEO satellite and accurately control signal emission at its output, in order to virtually eliminate the uplink and obtain GNSS-like signals with only the downlink SiS propagation effects.
- ✓ To do so in a way to maintain coherence (*i.e.* alignment) between code and carrier measurements, and to be compliant with ICAO standards and performance requirements.

Objectives

Objectives of this presentation

- To present the development of the Long Loop Algorithm (LLA) for NLES V3 stations and future EGNOS evolutions.
- To show MATLAB simulation results on the LLA performance and experimentation results with real hardware on Indra's platform.
- To present fulfillment of performance requirements according to ICAO Standards and Recommended Practices (SARPS) to show the goodness of the designed LLA.

Outline

1. Introduction and objectives
2. Problem statement
3. Architecture of the Long Loop Algorithm (LLA)
4. Estimation module and control module
5. Experimentation results and performance evaluation
6. Conclusions and on-going work

Uplink / downlink system overview at signal level

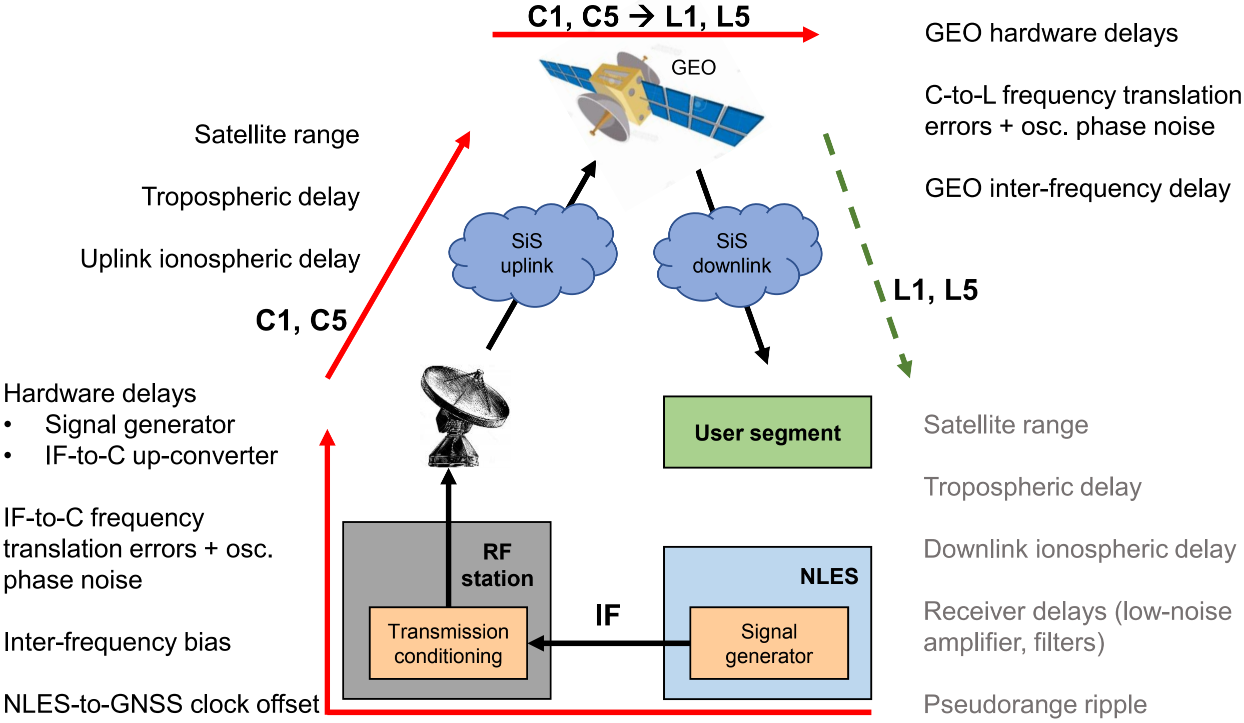

SPCOMNAV Signal Processing for Communications and Navigation
Universitat Autònoma de Barcelona School of Engineering UAB

Closing the loop with the Long Loop Algorithm

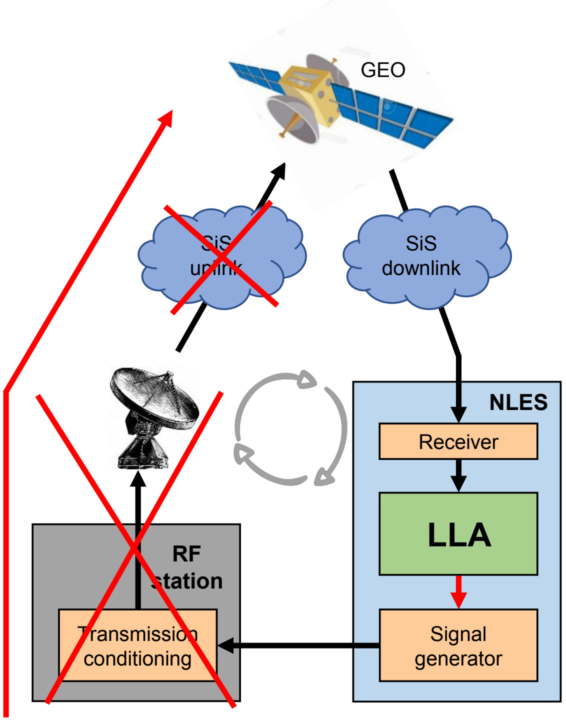

LLA OPERATION

1. Determination of the propagation effects in the uplink path from NLES to GEO.

2. Compensation for the identified effects by applying chip rate and carrier frequency controls into the NLES signal generator.

Outline

Architecture of the Long Loop Algorithm

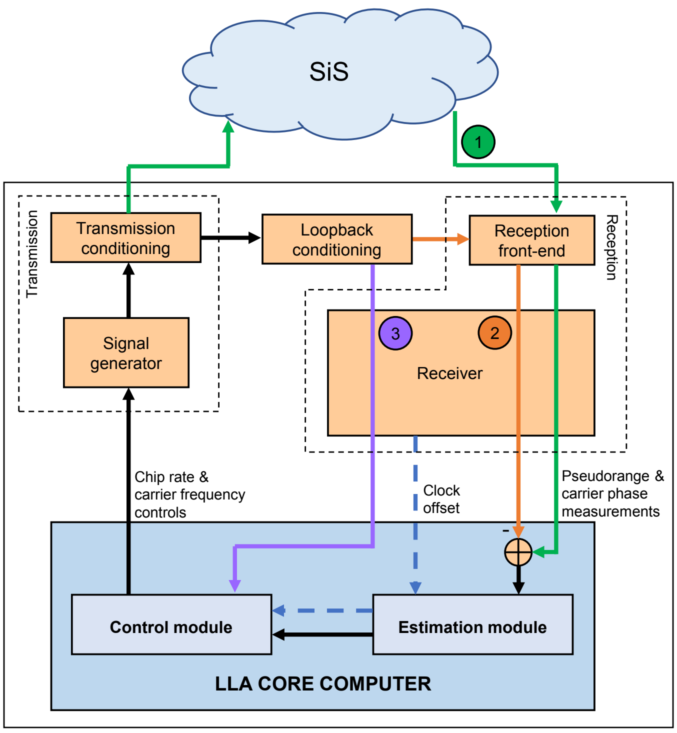

- The **long loop (1)** carries the delays and SiS propagation effects to be determined + applied corrections
- The **middle loop (2)** is used to:
  - ✓ Allow estimation module to perceive SiS independently from corrections applied at signal generator.
  - ✓ Subtract effects at the receiver side that are not to be corrected, and thus must not enter the LLA loop.
- The **short loop (3)** is used to:
  - ✓ Retrieve transmission effects to be corrected but lost during (1) – (2).
  - ✓ Retrieve information on the corrections that are actually applied and know what remains to be corrected.

Outline

Estimation module

- A **Kalman filter** is used to dissociate the different delays and propagation effects.

INPUT MEASUREMENTS (noisy)

Pseudorange and carrier phase measurements

$\rho_{L1}, \rho_{L5}, \varphi_{L1}, \varphi_{L5}$

- Satellite range + tropospheric delay + aggregate hardware delays
- Ionospheric delay (downlink, L1) (all other delays are obtained from this one through scaling factors)
- (Accumulated) frequency translation error at L1 (error at L5 obtained through scaling factor)
- Aggregate inter-frequency bias
- Carrier phase ambiguities
- Pseudorange ripple at L1 (pseudorange ripple at L5 is negligible)

Clock offset measurements → NLES-to-GNSS clock offset + drift

OUTPUT
State vector

$$\begin{bmatrix} \boxed{r(n)} \\ \dot{r}(n) \\ \ddot{r}(n) \\ \boxed{I_{L1}(n)} \\ \dot{I}_{L1}(n) \\ \ddot{I}_{L1}(n) \\ \boxed{\theta_{L1}(n)} \\ \dot{\theta}_{L1}(n) \\ \boxed{b_{L1L5}} \\ K_{L1} \\ K_{L5} \\ o_{L1}(n) \\ \dot{o}_{L1}(n) \\ \ddot{o}_{L1}(n) \\ \boxed{b_{clk}(n)} \\ d_{clk}(n) \end{bmatrix} \doteq \mathbf{x}(n)$$

Features of the LLA V3 Kalman filter

$$\hat{\mathbf{x}}(n+1) = \mathbf{F} \cdot \hat{\mathbf{x}}(n)$$ → State transition equation

Transition matrix

$$\mathbf{F} \doteq \begin{array}{c} \begin{array}{cccccccc} r(n) & L_{L1}(n) & \theta_{L1}(n) & b_{L1L5} & K_{L1} & K_{L5} & o_{L1}(n) & b_{clk}(n) \end{array} \\ \begin{bmatrix}
1 & 1 & 1/2 & 0 & 0 & 0 & 0 & 0 & 0 & 0 & 0 & 0 & 0 & 0 & 0 & 0 \\
0 & 1 & 1 & 0 & 0 & 0 & 0 & 0 & 0 & 0 & 0 & 0 & 0 & 0 & 0 & 0 \\
0 & 0 & 1 & 0 & 0 & 0 & 0 & 0 & 0 & 0 & 0 & 0 & 0 & 0 & 0 & 0 \\
0 & 0 & 0 & 1 & 1 & 1/2 & 0 & 0 & 0 & 0 & 0 & 0 & 0 & 0 & 0 & 0 \\
0 & 0 & 0 & 0 & 1 & 1 & 0 & 0 & 0 & 0 & 0 & 0 & 0 & 0 & 0 & 0 \\
0 & 0 & 0 & 0 & 0 & 1 & 0 & 0 & 0 & 0 & 0 & 0 & 0 & 0 & 0 & 0 \\
0 & 0 & 0 & 0 & 0 & 0 & 1 & 1 & 0 & 0 & 0 & 0 & 0 & 0 & 0 & 0 \\
0 & 0 & 0 & 0 & 0 & 0 & 0 & 1 & 0 & 0 & 0 & 0 & 0 & 0 & 0 & 0 \\
0 & 0 & 0 & 0 & 0 & 0 & 0 & 0 & 1 & 0 & 0 & 0 & 0 & 0 & 0 & 0 \\
0 & 0 & 0 & 0 & 0 & 0 & 0 & 0 & 0 & 1 & 0 & 0 & 0 & 0 & 0 & 0 \\
0 & 0 & 0 & 0 & 0 & 0 & 0 & 0 & 0 & 0 & 1 & 0 & 0 & 0 & 0 & 0 \\
0 & 0 & 0 & 0 & 0 & 0 & 0 & 0 & 0 & 0 & 0 & 1 & 1 & 1/2 & 0 & 0 \\
0 & 0 & 0 & 0 & 0 & 0 & 0 & 0 & 0 & 0 & 0 & 0 & 1 & 1 & 0 & 0 \\
0 & 0 & 0 & 0 & 0 & 0 & 0 & 0 & 0 & 0 & 0 & 0 & 0 & 1 & 0 & 0 \\
0 & 0 & 0 & 0 & 0 & 0 & 0 & 0 & 0 & 0 & 0 & 0 & 0 & 0 & 1 & 1 \\
0 & 0 & 0 & 0 & 0 & 0 & 0 & 0 & 0 & 0 & 0 & 0 & 0 & 0 & 0 & 1
\end{bmatrix} \end{array}$$

- ✓ Fulfillment of **system observability**.
  - ➢ Reduce from 7 to 4+3 estimated magnitudes by assuming zero initial offset in some states.
- ✓ Isolation of carrier phase ambiguities and pseudorange ripple for clean determination of states of interest.
- ✓ Independent clock offset filtering and further steering at measurement level.
- ✓ Kalman filter tuned for NLES+GEO oscillator phase noise tracking.
- ✓ **Prediction mode**. Rely on internal state-space model and provide service continuity when measurements are not received for some seconds due to hardware malfunction.

SPCOMNAV Signal Processing for Communications and Navigation
Universitat Autònoma de Barcelona School of Engineering UAB

Control module. Features

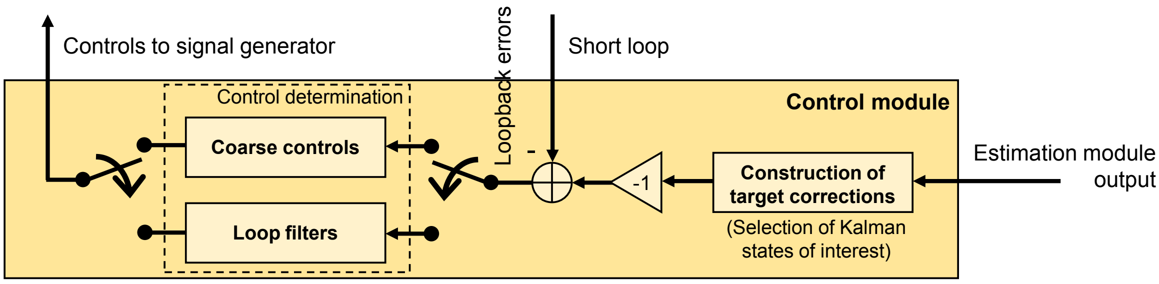

CONTROL MODULE STRATEGY

1. Convergence. Exploit maximum dynamic range of signal generator control inputs to quickly apply all coarse corrections, even if receiver loses lock.
2. Steady state. When receiver reacquires, switch to loop filters to filter out short-loop noise and smooth residual controls to ensure system stability.

CONTROL MODULE FEATURES

- ✓ Quick convergence.
- ✓ Intelligent determination of remaining corrections thanks to short loop.
- ✓ **Real-time steering** of time-varying propagation effects.
- ✓ **Prediction mode** (essential particularly during LLA convergence).

Outline

MATLAB simulation results

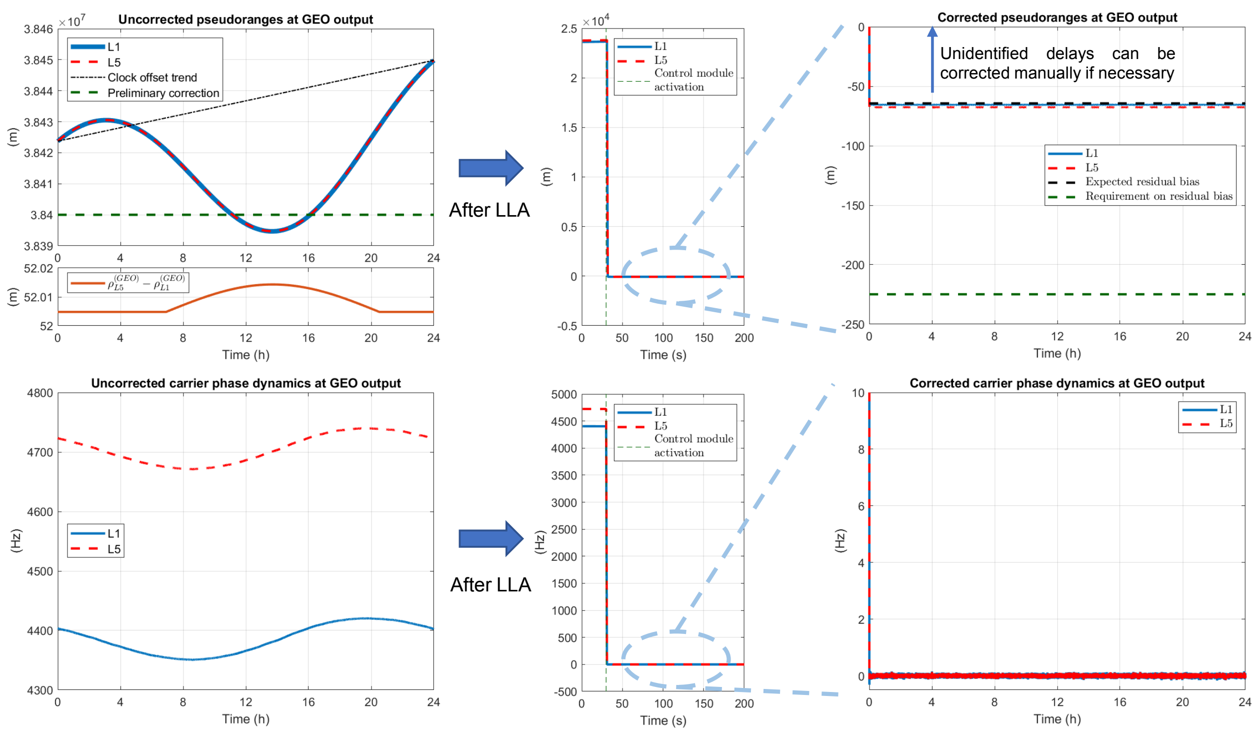

Experimentation results on Indra's platform

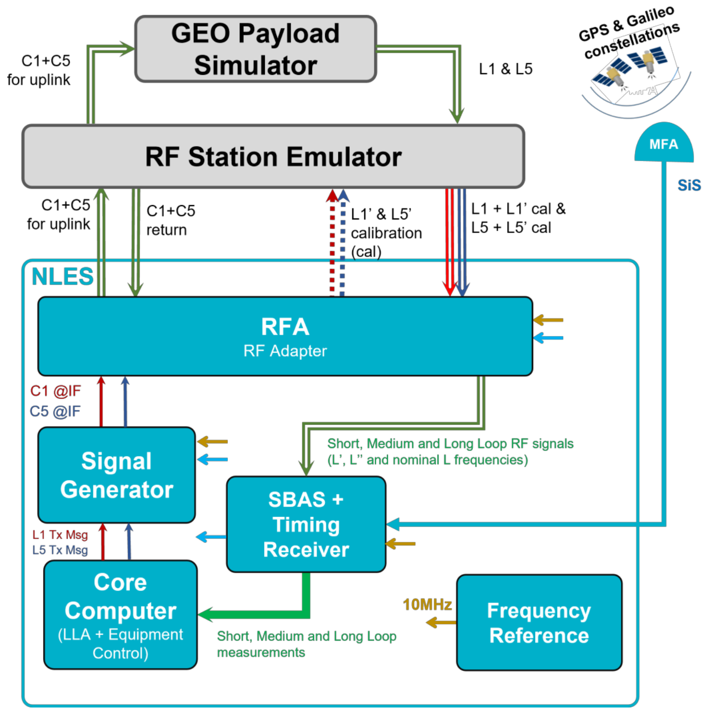

SPCOMNAV Signal Processing for Communications and Navigation
Universitat Autònoma de Barcelona School of Engineering UAB

Experimentation results on Indra's platform

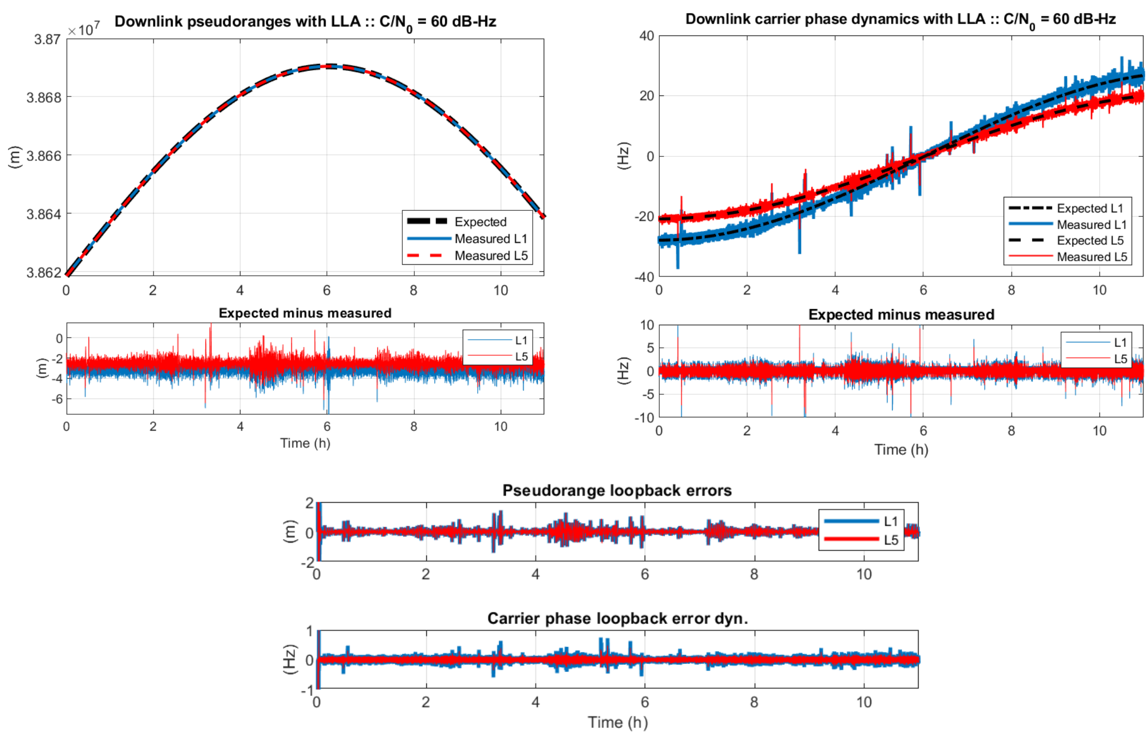

Fulfillment of ICAO performance requirements

ID	Threshold	MATLAB sim.	Indra's platform	Observations
Short-term CCC @L1	$< 0.150\ m$	$0.028\ m$	$0.035\ m$	-
Short-term CCC @L5	$< 0.200\ m$	$0.041\ m$	$0.028\ m$	
Long-term CCC @L1	$< 0.190\ m$	$0.059\ m$	$0.121\ m$	
Long-term CCC @L5	$< 0.255\ m$	$0.084\ m$	$0.108\ m$	
Short-term FreqCoh @L1	$< 5 \cdot 10^{-11}$	$1.366 \cdot 10^{-11}$	$1.784 \cdot 10^{-11}$	1-sigma
Short-term FreqCoh @L5		$1.957 \cdot 10^{-11}$	$1.489 \cdot 10^{-11}$	
Long-term FreqCoh @L1	$< 0.190\ m$	$0.087\ m$	$0.173\ m$	
Long-term FreqCoh @L5	$< 0.255\ m$	$0.125\ m$	$0.152\ m$	
LLA convergence	$< 120\ s$	N/A	$\sim 45\ s$	As soon as receiver reacquires

Acronyms:

- CCC Code-Carrier Coherence
- FreqCoh Code-Carrier Frequency Coherence

Outline

1. Introduction and objectives
2. Problem statement
3. Architecture of the Long Loop Algorithm (LLA)
4. Estimation module and control module
5. Experimentation results and performance evaluation
6. Conclusions and on-going work

Closure

CONCLUSIONS

- ❑ The designed LLA allows real-time tracking and steering of time-varying propagation effects to manipulate perceived downlink by controlling signal emission at output of GEO satellite.

- ❑ Main key-enabling features:
  - ✓ Fulfillment of Kalman filter observability.
  - ✓ Tracking and steering of clock offset and oscillator phase noise.
  - ✓ Fast LLA convergence.
  - ✓ LLA continuity in the absence of measurements for some seconds.

- ❑ Fulfillment of ICAO performance requirements.

- ❑ The proposed design of the Long Loop Algorithm is not only useful for EGNOS V3, but it also paves the path for future SBAS evolutions.

ON-GOING WORK

- ❑ On-factory testing with real hardware and GEO payload simulator.
- ❑ On-site testing with real GEO satellite slot planned this year.

SPCOMNAV Signal Processing for Communications and Navigation
Universitat Autònoma de Barcelona
School of Engineering UAB

Thank you for your attention!

THIS PAGE INTENTIONALLY LEFT BLANK